The effect of different chemical compositions caused by the variation of deposition potential on properties of Ni–Co films

Ali Karpuz [a,*], Hakan Kockar [a], Mursel Alper [b]

[a] *Physics Department, Science & Literature Faculty, Balikesir University, Balikesir, Turkey*
[b] *Physics Department, Science & Literature Faculty, Uludag University, Bursa, Turkey*

ARTICLE INFO

ABSTRACT

The magnetic and microstructural properties of Ni–Co films electrodeposited at different cathode potentials were investigated. The compositional analysis revealed that the Ni content increases from 13 at.% to 44 at.% in the films with increasing deposition potential. Magnetic measurements showed that the saturation magnetization, M_s of the films decreased with increase of Ni content as the deposition potential increased. M_s values changed between 1160 emu/cm^3 and 841 emu/cm^3. The X-ray diffraction revealed that the crystalline structure of the films is a mixture of the predominant face-centered cubic (fcc) and hexagonal closed packed. However, the mixture phase turns to the fcc because of increasing Ni content up to 44 at.% at the highest (-1.9 V) potential by enhancing the intensity of reflections from the fcc phase. The changes observed in the magnetic and microstructural properties were ascribed to the changes observed in the chemical composition caused by the applied different deposition potentials.

1. Introduction

Magnetic films are important materials for reading/writing heads, magnetosensors and magnetic data storage devices due to their capability and quality [1–3]. In recent years, comprehensive studies [2,4] on magnetic films have provided new potential applications where these films were used. Especially, Ni and Ni–Co have been produced with many techniques and largely studied to develop magnetic and magnetoresistive devices [5–7]. The electrodeposition is one of the popular techniques that are used to produce magnetic films and alloys [1,2,4,7–9]. In electrodeposition, experimental parameters such as deposition potential, electrolyte composition and thickness can change the properties of deposits [10,11]. In the present work, the characterizations of Ni–Co films prepared at different potentials were performed and the results of investigation were reported. The magnetic and structural properties were observed to have a strong dependence on the Ni:Co ratio that was controlled by the deposition potential.

2. Experimental

Ni–Co alloy films were electrodeposited from the electrolyte containing 0.4 M nickel sulfamate, 0.2 M cobalt sulfate and 0.2 M boric acid at the deposition potentials of -1.1 V, -1.3 V, -1.5 V and -1.9 V. A potentiostat/galvanostat (EGG model 362) was controlled with a computer potentiostatically and an electrochemical cell with three electrodes was served for deposition of the films. The platinum foil was used as anode, the titanium (Ti) substrates as cathode and saturated calomel electrode (SCE) as the reference electrode. All potentials were with respect to the SCE. Deposition of the films was realized at room temperature from the unstirred aqueous solution and the thickness of the deposits was fixed at 3 μm by the aid of a computer that was programmed according to Faraday's Law. After deposition, the films were peeled mechanically from their substrates and stored in proper conditions for characterizations.

The cyclic-voltammogram (CV) curve of the electrolyte was procured before deposition of the films. The scans were performed by using Ti electrode as cathode and scanning the potential from +1.0 V to -1.5 V with a potential scan rate of 20 mV/s. During growth process, the current was also recorded as a function of time to study the deposition process of the Ni–Co alloys.

The compositional analysis of the films was done by the energy dispersive X-ray spectroscopy (EDX, GENESIS APEX 4 – EDAX, AMETEK) at the same time with the investigation of surface morphology. The EDX measurements were achieved by inserting a small part of film on sample holder with conductive adhesive tape. The hysteresis loops of films were obtained from the vibrating sample magnetometer (VSM, ADE technologies DMS-EV9 Model,) by scanning the magnetic field between ±10 kOe at room temperature. The structural analysis of the films was made with the X-ray diffraction (XRD, PANalytical) technique by using Cu-K$_\alpha$ radiation between 40° and 100° with the step size of 0.02°. Surface morphology of

* Corresponding author at: Balıkesir Üniversitesi Fen Edebiyat Fakültesi Çağış Yerleşkesi 10145 Balıkesir. Tel.: +90 266 6121278; fax: +90 266 6121215.
E-mail address: alikarpuz@bau.edu.tr (A. Karpuz).
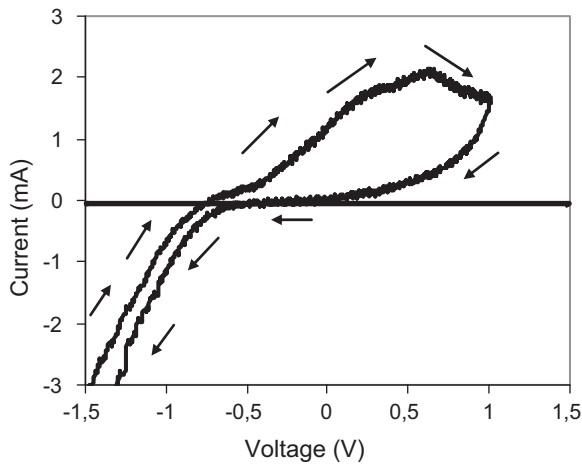
Fig. 1. The CV curve of the electrolyte used for deposition of Ni–Co films.

the films was investigated with the scanning electron microscope (SEM, FEI™, NOVA NANOSEM 430).

3. Results and discussion

The electrolyte was characterized by using the CV to find the appropriate region of deposition potential. The CV curve of the electrolyte used for the deposition of Ni–Co films is given in Fig. 1. As seen, after about −0.8 V, the current suddenly began to increase. This corresponds to the ion deposition occurred on the cathode surface. When the scan was reversed, a broad anodic peak was seen at around 0.5 V. This peak might be caused by dissolution of the Ni or Co atoms. Beside, deposition potential values from −0.5 V up to −1.0 V were applied to confirm the CV results and it was shown that no proper deposits and film structure formed in this potential region for characterization. According to observations, the deposition potential range of the Ni–Co films was selected to be between −1.1 V and −1.9 V considering the potentiodynamic measurements and also the film appearance.

The current–time transients were also recorded during the deposition process in order to control the stability of deposition as in [12]. The current–time transients for the films grown at different deposition potentials are given in Fig. 2. It was clearly seen that the current occurred between anode and cathode in the electrolyte increased as the deposition potential increased. It was understood
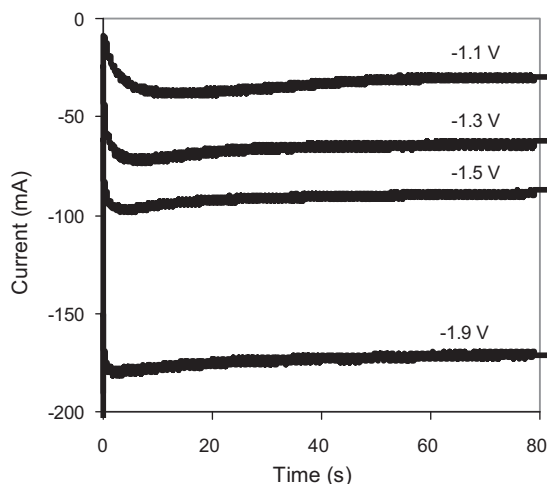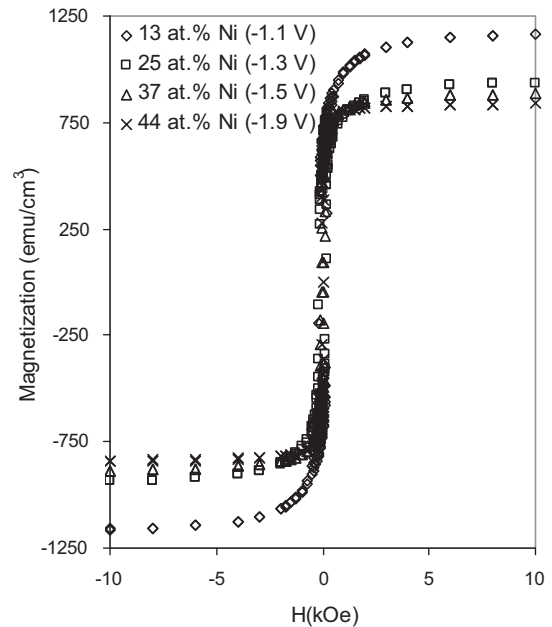

Fig. 3. The hysteresis loops of the films produced at the different potentials.

that the films were deposited correctly and uniformly since the current values were almost stable for each deposition potential as can be seen in Fig. 2.

The compositional analysis of the films by EDX showed that the films consist of ∼13 at.%, ∼25 at.%, ∼37 at.% and ∼44 at.% Ni and ∼87 at.%, ∼75 at.%, ∼63 at.%, ∼56 at.% Co for the films deposited at −1.1 V, −1.3 V, −1.5 V and −1.9 V, respectively. The result means that the Ni–Co films grown in this potential range present anomalous codeposition because of the reason which was explained in [7]. The anomalous codeposition was also reported for two different current densities in [7].

The hysteresis loops of the films grown at different potentials are shown in Fig. 3. The saturation magnetization, M_s, and the coercivity, H_c, values were drawn as a function of Ni content of the films in Fig. 4. The highest M_s was at the lowest deposition potential as ∼1160 emu/cm^3 corresponding to the low (13 at.%) Ni content and the M_s continued to decrease gradually to the lowest value (∼841 emu/cm^3) since the Ni content of the films increased to the
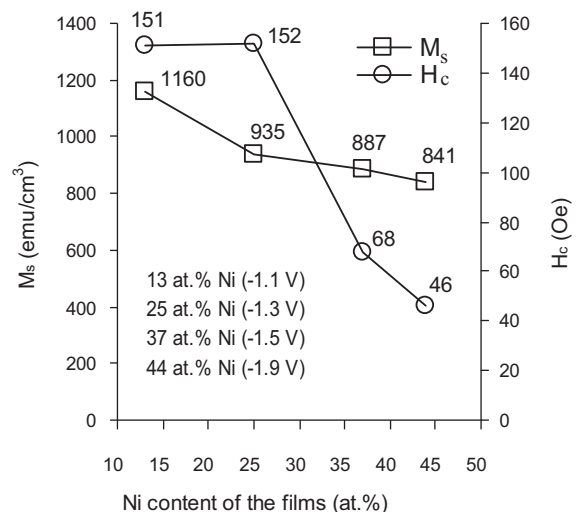

Fig. 2. The current–time transients of the Ni–Co films grown at the different deposition potentials.

Fig. 4. Variation of the M_s and H_c values as a function of Ni content for the Ni–Co films grown at the different deposition potentials.
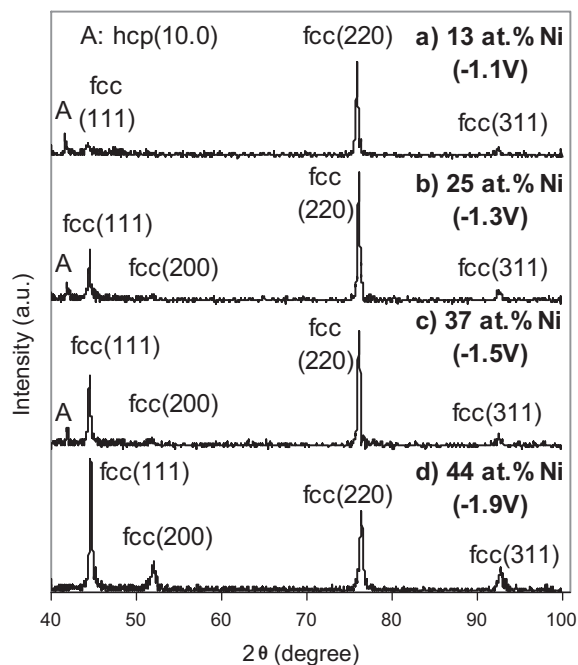
Fig. 5. XRD patterns of the films grown at the different deposition potentials.

44 at.% at the highest potential. The M_s values decreased with the increase of potential and were found between 1420 emu/cm^3 of the bulk Co and 480 emu/cm^3 of the bulk Ni [13]. H_c values of the films changed between 152 Oe (±1 Oe) and 46 Oe (±1 Oe) as the Ni content increased from 13 at.% to 44 at.%. It is easy to magnetize the Ni–Co films deposited at high potentials since the soft magnetic properties of the films increased with the decrease of the H_c with increasing Ni content. The results are in agreement with the compositional dependence of M_s and H_c in other work [14].

XRD patterns of all Ni–Co films were illustrated in Fig. 5. The results obtained from the XRD measurements revealed a mixed crystalline structure consisting of mostly predominant face-centered cubic (fcc) and the hexagonal closed packed (hcp) structures. In the patterns, the (1 1 1), (2 0 0), (2 2 0) and (3 1 1) reflections of the fcc structure are at the angular position of $2\theta \cong 44°$, 51°, 76° and 92°, respectively. Beside, the films have the (10.0) peak of hcp structure (labeled as A in Fig. 5) from the Co at $2\theta \cong 41°$ except for the film which contains 44 at.% Ni and deposited at −1.9 V. It is clearly seen that the intensity of the hcp (10.0) peak decreases and the peaks of fcc become more dominant for the mixture structures as the Ni content of the films increases. Mixed crystalline structure of the fcc + hcp turned to the fcc phase since the peak occurred at $2\theta \cong 41°$ is missing from the XRD pattern of the film which contains 44 at.% Ni. Similar change in crystalline structure depending on alloy composition was also detected in earlier studies [15,16]. The preferential texture of the films calculated from the relative peak intensities of the XRD patterns [17] was the (2 2 0) fcc orientation. The average values of the grain sizes of crystallites determined by using the Scherrer formula [7,18] were between ∼26 nm and ∼39 nm. The recent work [7] reported that the average grain sizes of electrodeposited Ni–Co alloys were around 10 nm for all electrolyte concentration range. The differences of grain sizes between present work and [7] may be due to different substrates and chemicals which were used during the deposition of films.

Fig. 6 shows the SEM micrographs of the Ni–Co films deposited at different potentials. It was clearly seen from the figure that the surface homogeneity decreased when the deposition potential increased. More homogeneous surfaces piled with a large number of equally sized grains were observed from SEM images of the films
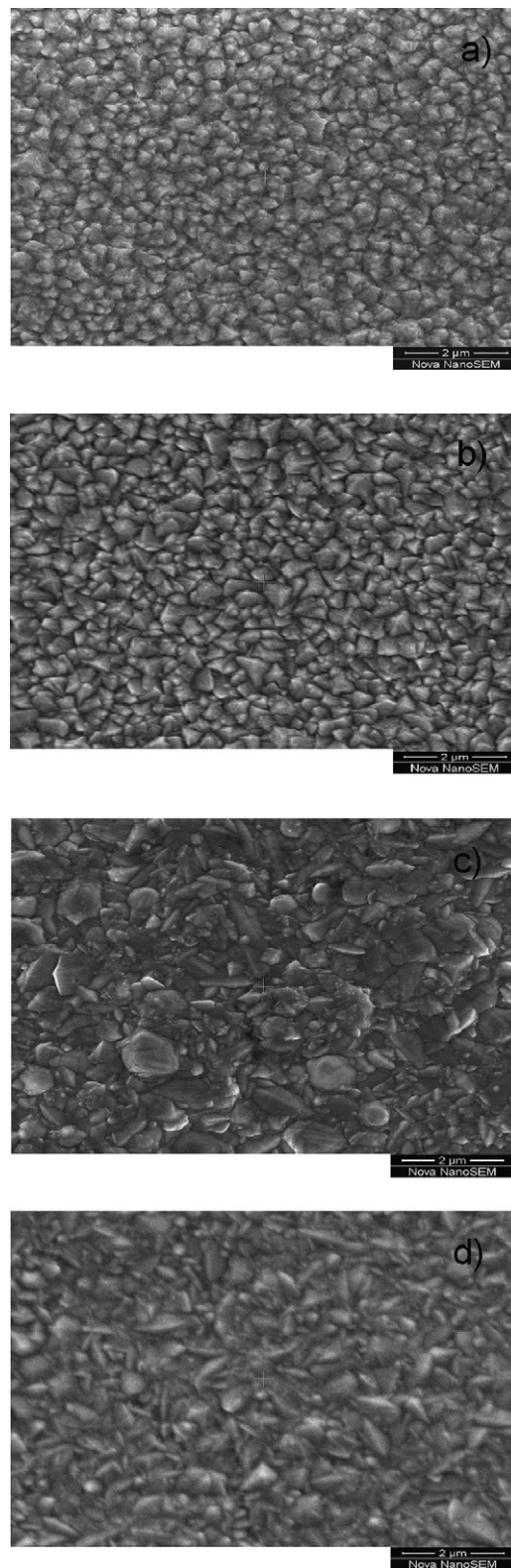
Fig. 6. SEM micrographs of the Ni–Co films deposited at the different deposition potentials, (a) −1.1 V (13 at.% Ni), (b) −1.3 V (25 at.% Ni), (c) −1.5 V (37 at.% Ni), (d) −1.9 V (44 at.% Ni).

deposited at −1.1 V (13 at.% Ni) and −1.3 V (25 at.% Ni), see Fig. 6(a) and (b), compared to that of the films deposited at −1.5 V (37 at.% Ni) and −1.9 V (44 at.% Ni) as seen in Fig. 6(c) and (d). When the Ni content increased to 37 at.% and 44 at.%, the morphology of the Ni–Co films changed dramatically and surface appearance turned to pebbly structure.

4. Conclusions

A series of the Ni–Co films was deposited at the different deposition potentials and their magnetic and structural properties were studied. Ni content of the films increased gradually as the deposition potential was changed from the −1.1 V to the −1.9 V. Magnetic measurements indicated that M_s decreased as the deposition potential increased. The films consist of mostly a mixed predominant fcc and hcp phase, and the peak intensities of the fcc fraction increased with the decrease of the hcp (10.0) peak due to increasing Ni content as the potential increased. Thus, the differences in the magnetic and structural properties of the films may be attributed to the compositional differences caused by the variation of the deposition potential.

Acknowledgments

References

[1] A. Dolati, S.S. Mahshid, Materials Chemistry and Physics 108 (2008) 391.
[2] W. Schwarzacher, D. Lashmore, IEEE Transactions on Magnetics 32 (1996) 3133.
[3] S. Bagchi, S. Anwar, N.P. Lalla, Applied Surface Science 256 (2009) 541.
[4] J. Gong, W.H. Butler, G. Zangari, IEEE Transactions on Magnetics 41 (2005) 3634.
[5] J.B. Yi, Y.Z. Zhou, J. Ding, G.M. Chow, Z.L. Dong, T. White, A.T.S. XingYu Gao, X.J.Yu Wee, Journal of Magnetism and Magnetic Materials 284 (2004) 303.
[6] S.U. Jen, C.C. Liao, Journal of Alloys and Compounds 270 (1998) 73.
[7] B.G. Toth, L. Peter, A. Revesz, J. Padar, I. Bakonyi, European Physical Journal B 75 (2010) 167.
[8] M. Srivastava, V.K.W. Grips, K.S. Rajam, Applied Surface Science 257 (2010) 717.
[9] L. Sziráki, E. Kuzmann, M. El-Sharif, C.U. Chisholm, S. Stichleutner, G.B. Lak, K. Süvegh, E. Tatára, Z. Homonnay, A. Vértes, Applied Surface Science 256 (2010) 7713.
[10] M. Safak, M. Alper, H. Kockar, Journal of Magnetism and Magnetic Materials 304 (2006) e784.
[11] M. Alper, H. Kockar, M. Safak, M.C. Baykul, Journal of Alloys and Compounds 453 (2008) 15.
[12] A Karpuz, H. Kockar, M. Alper, European Physical Journal Applied Physics 48 (2009) 30504.
[13] D. Jiles, Introduction to Magnetism and Magnetic Materials, Chapman and Hall, London, 1996.
[14] D. Kim, D.-Y. Park, B.Y. Yoo, P.T.A. Sumodjo, N.V. Myung, Electrochimica Acta 48 (2003) 819.
[15] E. Gómez, S. Pané, E. Vallés, Electrochimica Acta 51 (2005) 146.
[16] L. Wang, Y. Gao, Q. Xue, H. Liu, T. Xu, Applied Surface Science 242 (2005) 326.
[17] A. Vicenzo, P.L. Cavallotti, Electrochimica Acta 49 (2004) 4079.
[18] B.D. Cullity, Elements of X-Ray Diffraction, 2nd. ed., Addison-Wesley, USA, 1978.